Measurement of ultra-high energy cosmic rays by the Telescope Array experiment

M.Fukushima on behalf of the TA Collaboration
Institute for Cosmic Ray Research, University of Tokyo

The Telescope Array (TA) is a cosmic ray experiment in Utah, USA for the measurement of ultra-high energy cosmic rays (UHECRs). The construction of TA started in 2003, and was completed in March 2008. The design and performance of TA, its data analysis and preliminary physics results are reported.

1. Introduction

A cutoff structure is expected in the energy spectrum of UHECRs around 10^{20}eV. It originates from the interaction of cosmic ray protons with the cosmic microwave background and was predicted by Greisen, Zatsepin and Kuzmin (GZK) in 1966[1]. Since that prediction, the search for the GZK cutoff became one of central themes in the study of UHECRs.

The Akeno Giant Air Shower Array (AGASA) is an array of 111 scintillator Surface Detectors (SDs) covering the ground area of $\sim$100km^2 in Akeno, Japan[2]. The AGASA reported an energy spectrum extending beyond the predicted GZK cutoff in 1998[3]. A total of 11 events was observed above 10^{20}eV with an exposure of 1.62×10^3 km^{2}sr yr where only less than 3 events were expected if the GZK cutoff was there according to the final report in 2003[4].

The AGASA result was contradicted by the High Resolution Fly's Eye (HiRes) in the 27th International Cosmic Ray Conference (ICRC) in Hamburg in 2001. The HiRes used a newly developed air fluorescence technique[5] and demonstrated the existence of the cutoff at the energy of $10^{19.75}$eV where the GZK cutoff is expected. According to the final result published in 2008[6], the number of events observed above $10^{19.8}$ eV was 13 whereas the extended spectrum without the cutoff predicted 43.2 events.

In the search for the origin of UHECRs, AGASA and HiRes had been collaborating to build a large array of fluorescence telescopes (TA) in Utah[7]. The apparent contradiction on the spectrum had triggered a serious discussion in the collaboration. It became soon apparent that the systematic biases in both measurements have to be thoroughly understood before committing to build a full-scale TA. The first phase of TA was proposed in 2002 to understand the difference of AGASA and HiRes by locating the AGASA type ground array and the HiRes type fluorescence telescopes on the same experimental site, and by cross-calibrating each other. The phase-1 TA was funded in 2003 and the construction started.

Meanwhile the construction of the Pierre Auger Observatory (PAO) had been proceeding in Argentina since 1999. The PAO is a hybrid experiment employing $\sim$1600 water tank SDs covering the area of 3,000km^2 together with 4 stations of fluorescence detectors (FDs) overlooking the SD area[8]. The PAO group published an energy spectrum in 2008[9] based on the data collected since 2004 by using a part of the completed detectors. The spectrum shows the break in power law at 4×10^{19}eV and the flux above was strongly suppressed. The single power law passing the GZK cutoff was excluded with a significance of 6σ.

2. TA Detector

The detector configuration of TA is shown in Fig.1. The SD covers the ground area of 680 km^2 and has an aperture of $\sim$1,600 km^{2}sr (θ <60°). The FD has a stereoscopic aperture of $\sim$1,000 km^{2}sr at 10^{20}eV with a duty factor of approximately 10%. It is located 140 miles south of Salt Lake City (lat. 39.3°N, long. 112.9°W) in the West Desert of Utah with an average altitude of 1,400m.

2.1. Surface Detector

The SD consists of 507 plastic scintillators of 3m^2 large deployed in a grid of 1.2km spacing. Each SD is composed of two layers of plastic scintillator overlaid on top of each other with a stainless steel sheet of 1mm thickness in between. The scintillator is 1.2cm thick and is read out by 96 wave length shifting fibers installed in the grooves on the surface. Both ends of the fibers were connected to a PMT and two layers were read out independently by two PMTs. A passage of a cosmic ray muon gives 24 photo-electrons on average to one PMT.

The signal from each PMT is continuously digitized and recorded by a 12-bit flash ADC with 50MHz sampling. The timing of the clock is synchronized with a pps signal generated by the global positioning system (GPS) at each SD. The accuracy of GPS relative timing is better than 20ns. The recording of the PMT waveform enables a reliable determination of the deposited charge and the particle timing by measuring the distribution of particles inside the shower disk.

One of the SDs deployed in the field is shown in Fig.2. All SDs are autonomously operated in the field

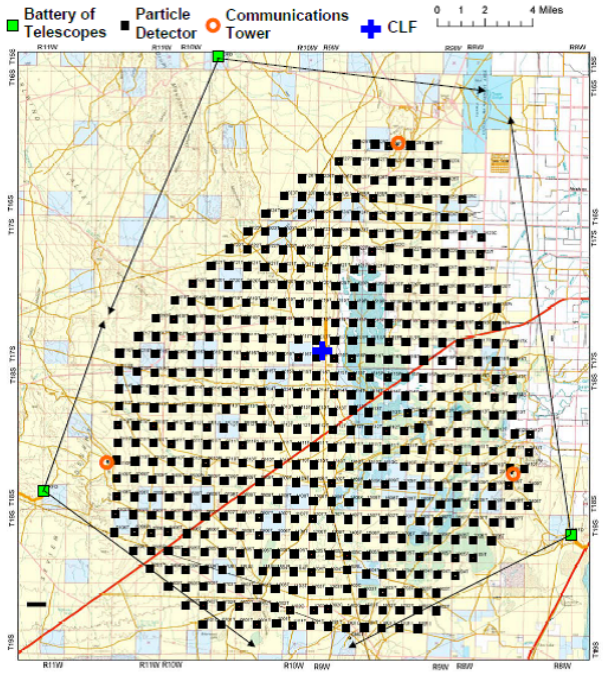

Figure 1: Detector configuration of phase-1 TA. The black squares indicate the locations of SDs and the green squares indicate FD stations. The orange circles are communication towers.

Figure 2: One of the SDs deployed in the Field.

without any utility wires. The average power consumption of ∼7W is locally provided by the solar panel of 120W and a backup battery. A communication for the trigger and the waveform collection is achieved using 2.4GHz wireless LAN modem.

Approximately 80% of the SDs are on the federal land, ∼10% on the Utah state trust land and the rests are on privately owned lands. The whole SD assembly weighs ∼640kg and it made the deployment and the maintenance by helicopter possible without disturbing the flora and fauna of the wilderness.

Table I Definition of SD Trigger

Level	Definition	Rate	Function
0	$Q>0.3Q_\mu$	∼700Hz	waveform storage
1	$Q>3Q_\mu$	∼25Hz	"hit" definition
2	adjacent 3 "hits"	∼0.01Hz	"event" definition

The data acquisition trigger is formed in 3 levels as shown in Table I, where Q_μ means the average charge deposited by a cosmic ray muon penetrating the SD. The level-0 trigger is caused by the upper and lower scintillators in coincidence, and the level-1 trigger requires either of the scintillators satisfies the condition. Each SD stores the waveform locally by the level-0 trigger. A timing table of level-1 hits is assembled by the master PC at the communication tower for every second and the level-2 decision is made. The level-2 requires at least 3 adjacent SD hits within 8μs. The level-2 trigger decision is broadcasted to all the SDs from the tower and the stored waveform within $\pm32\mu$s of the level-2 timing is picked up and transferred to the tower. Free time slots between the trigger communications are used for the waveform transfer. The data acquisition of the SD is pipelined and is dead time free.

The whole SD array was initially configured by 3 sub-arrays of 100, 193 and 207 SDs, each of which was controlled by the master PC at the communication tower. By the end of May 2008, after overcoming the multipath interference and problems caused by wild or domestic animals in the field, a stable data collection was achieved with 3 sub-arrays operated independently. In November 2008, we added 7 more SDs to complete the array, and at the same time integrated 3 sub-arrays into one by introducing the border (of sub-array) crossing trigger. The DAQ up time since May 2008 is ∼97% with approximately 99% of the SDs online and properly functioning.

The pulse height spectrum by the level-0 trigger is histogrammed at each SD and readout every 10 minutes (Fig.3) together with DAQ and environment monitoring parameters. This enables us to track the gain of each SD with an accuracy of ∼1% every 10 minutes. The linear range of the SD is checked by accumulating the spectrum for longer duration (minimum 4 days) and checking a specific distortion at the high energy end. The response is linear within 5% for the arrival of approximately 150Q_μ at the same time. An example of high energy SD event is shown in Fig.4.

2.2. Fluorescence Detector

One of the FD stations, the Middle Drum (MD) station in the north, is built by the transfer of the HiRes detector[5]. Fourteen HiRes telescopes and HiRes-I

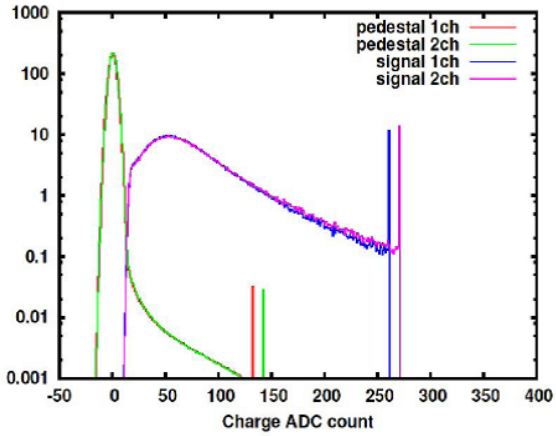

Figure 3: A muon spectrum obtained by the SD. A total of ∼420k muons is accumulated every 10 minutes for each SD.

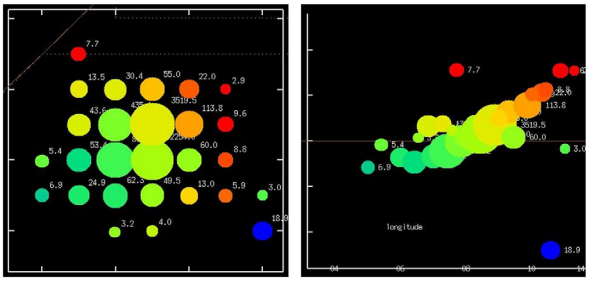

Figure 4: An example of large SD event; a plan view (left) and a side view (right). The radius of the hit circle is proportional to the logarithm of detected charge. The hit timing is color coded. In the right figure, the vertical axis is in the hit timing

sample and hold electronics are used. This FD station serves as an "anchor" for the comparison of the energy scale between the old (HiRes) and the new (TA) experiments. Below, the design and performance of newly produced FDs at 2 other locations in the south, Black Rock Mesa (BRM) and Long Ridge (LR), are reported.

A battery of 12 reflector telescopes covers the sky of 3°–34° in elevation and 108° in azimuth at BRM and LR(see Fig.5). The mirror is a spherical dish of 6.8m^2 area and is composed of 18 segment mirrors of hexagonal shape. The curvature of the segment mirror is 6,067mm [7]. The direction of each segment mirror was individually adjusted and a spot size of less than 30mm in diameter was realized at the center of the focal plane. The reflector area is ∼30% larger than that of the HiRes telescope.

The air shower image is recorded by a mosaic PMT camera on the focal plane. A set of 16×16 PMTs with a hexagonal window is used for the camera. Each

Figure 5: Fluorescence detector station at BRM.

PMT covers a 1.1°×1.0° patch of the sky. A UV transmitting glass filter (BG3 by Schott) is attached in front of the PMT for reducing the night sky background. The whole camera is assembled in a chassis with a window made by the UV transparent plexiglass.

A negative high voltage is applied to each PMT and the gain (∼10^5) was individually adjusted. A measurement range is limited to ∼9,000 photo-electrons in 100ns by the FADC overflow. No significant deviation from the linearity is expected for the PMT and preamplifier in this range. The use of DC coupling enables a direct measurement of the night sky background. The signal of long duration from the distant shower, or by the laser shot, is recorded without distortion inherent to the AC coupling.

The signal from the PMT is amplified by a factor of 50 by the pre-amplifier and is sent to a digitizer electronics with a 12-bit, 40MHz flash ADC, where a trace of fluorescence signal is searched in pipeline by the sliding sum in the Field Programmable Gate Array (FPGA). The DC component (pedestal) is averaged over 1.4ms and is digitally subtracted. The waveforms of all 256 PMTs are read out and recorded by the PC when a cluster of adjacent 5 PMTs are fired with the S/N greater than 6[10].

All 3 FDs stations were installed by November, 2007 and started taking data. A stable trigger rate of ∼2 Hz is achieved at BRM and LR with ∼6% dead time after struggling with the noise caused by the commercial airplane flying over the TA sight. An example of the event is shown in Fig.6.

2.3. FD Calibration

For the new FDs at BRM and LR, 2 or 3 standard PMTs are installed in each camera. The gain of the standard PMT was calibrated in the laboratory using the light source of known intensity before installing into the camera. The Rayleigh scattered photon from the pulsed nitrogen laser was used as the

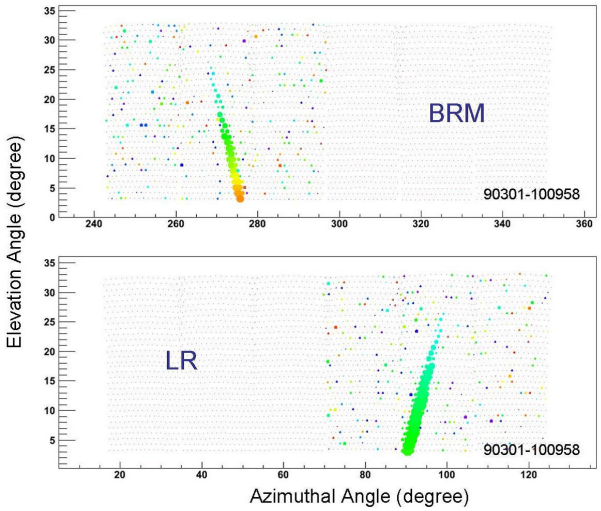

Figure 6: A stereo FD event. Event pictures from BRM and LR are shown. Both FD stations are separated by ∼ 40km. The radius of the circle is proportional to the logarithm of detected photoelectrons. The hit timing is color coded.

absolute intensity light source (∼8% accuracy) for this calibration. A tiny YAP($YAlO_3$:Ce) scintillator with ^{241}Am source was attached to the standard PMTs for monitoring the gain after the calibration. The gains of all other PMTs in the camera are adjusted in situ with respect to the standard PMT by using a diffused Xenon flasher pulse installed at the center of the reflector mirror[11]. A roving Xenon flasher developed by the HiRes group was also used to check the relative gain settings of all 3 stations.

An integrated end-to-end calibration is needed to confirm the energy scale of the FD measurement. We installed a small electron linear accelerator 100m away from the FD station (BRM). An electron beam vertically released into the atmosphere from the accelerator will be used for the FD calibration. A beam of 10^9 electrons with an energy of 40 MeV and a duration of 1μs simulates a shower energy deposition of $\sim 4\times10^{16}$eV[12]. An absolute accuracy significantly better than 10% will be achieved by comparing the observed fluorescence signal with the expected energy deposition.

A lidar system is being used at BRM site for the atmospheric monitoring. It consists of a pulsed laser (Nd:YAG, 355nm) and a telescope attached to an alt-azimuth mount. The laser is fired vertically and horizontally, and the back-scattered light is received by the telescope. The measurement was done before and after the FD observation. The data are analyzed to obtain the extinction coefficient along the path of the laser.

3. Data Analysis

In the following, data analyses for the spectrum using SD/FD hybrid events[13] and for the composition using stereo FD events are presented[14].

3.1. FD reconstruction

The air fluorescence signal is identified by integrating the PMT waveform after subtracting the online-recorded dc level. Signals with a S/N ratio larger than 3 are accepted for the reconstruction, where the noise was determined from the spread of the dc level. In order to determine the shower detector plane (SDP) of the event, signals satisfying the geometrical and temporal conditions are further assembled iteratively in the track recognition program. The SDP was calculated by averaging all the selected PMTs with a weight of the integrated signal size.

After event geometry is determined (in the stereo FD and SD/FD hybrid analyses described below), the size and the longitudinal development of the shower were determined by the inverse Monte Carlo (MC) method. The shower of certain size and the longitudinal shape was produced on the determined geometry and the expected signal size calculated by the MC ray tracing program was compared with the actual measurement at each PMT. The Gaisser-Hillas(GH) formula is used for simulating the longitudinal development of the energy deposit in the atmosphere, and the value of the shower maximum, X_{max}, is changed to match the data. The size and the X_{max} of the shower giving the maximum likelihood are chosen.

All the calibration and performance figures such as the air fluorescence yield, geometry and optics of the telescope, gain of the PMT and electronics, atmospheric attenuation and the contribution from the direct and scattered Cherenkov light are included in the MC to match the data. Specifically, we used the spectrum of the air fluorescence from the FLASH experiment[15] and the absolute yield of the air fluorescence by Kakimoto et al.[16].

3.2. Energy Spectrum

Events triggered by SD and FD independently are matched together time-wise and are analyzed as a single event. The trigger timings in SD and FD are required to be within 200 μs to originate from an identical event. An SDP is determined by the analysis of FD data as described above, and the core location and the shower axis elevation angle (Ψ) are determined by the timing fit of all FD hits and one SD hit. The planer shower front is assumed and a single SD hit giving the best χ^2 was chosen. After determining the shower geometry, the shower size and the X_{max} are fitted. A total of 124 events is selected for $E > 10^{18.65}$eV and

Table II Uncertainty of energy determination

item	% error
Air fluorescence yield	12%
Telescope calibration	10%
Atmospheric correction	11%
Unknown primary composition	5%
Reconstruction and missing energy	3%
TOTAL (added in quadrature)	19%

$\theta < 45^\circ$ from the data sample taken for May 2008 – September 2009.

The fitted GH-function was integrated to obtain the total calorimetric energy. It was then compared with the primary energy and the difference was corrected. This correction includes the effect of missing energy, which is carried by the neutral particles such as the neutrinos and the high energy muons propagating deeper into the ground (than the assumed GH shape of the calorimetric energy). The CORSIKA and COSMOS air shower codes, as well as several different hadronic interaction models were used to estimate the missing energy and its ambiguity. The uncertainty of the energy scale is 19% in total and the breakdown is given in Table II.

Hybrid Monte Carlo events were generated by COSMOS air shower MC using QGSJET–II with an energy spectrum of $E^{-3.1}$. The calibration and the detector condition of the actual detectors were used for the MC generation. The trigger efficiency and the event acceptance were estimated by analyzing these MC events using the same programs used for the data analysis. The energy resolution was found to be ∼8% over the measured range, and its influence on the flux was checked to be negligible.

The resultant spectrum multiplied by E^3 is shown in Fig.7. The obtained hybrid spectrum is consistent with that obtained by the Middle Drum (MD) telescope[17], and with the HiRes monocular and stereo measurements[6]. The result by Pierre Auger Observatory[9] seems to give systematically lower flux, or lower energy scale(∼25%). Likewise, the energy of AGASA[4] seems higher than ours by ∼20%. The obtained spectrum has no statistical power yet to check the flux suppression, or the extension, claimed by previous experiments in the energy region of $10^{19.6-20.0}$eV.

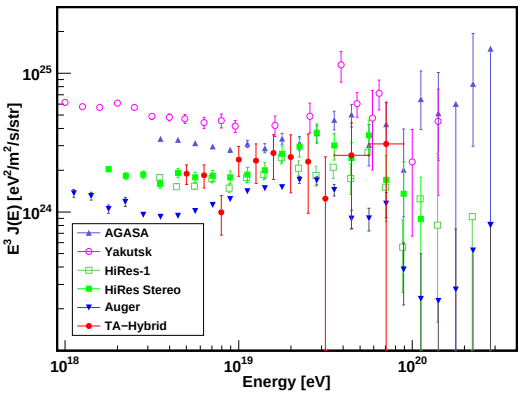

Figure 7: Energy spectrum obtained by analyzing SD/FD hybrid events. A Preliminary Result.

3.3. Composition

The value of X_{max} is known to be effective to differentiate the composition of arriving cosmic rays. The events falling in the central region of TA, and detected by 2 FD stations (BRM and LR), were used for the analysis of X_{max}. The SDP was determined at each FD station and the event geometry (shower axis) was defined as the intersect of two SDPs. The shower size and the X_{max} were optimized by the inverse MC method using the data of two FD stations simultaneously. Following cuts were applied for well reconstructed events;

- X_{max} is in the Field of view (FoV) of the telescope.
- The location of the shower core is in the circular area of radius 9.6km centered at the middle point of 2 FD stations.
- The energy and the zenith angle requirements are; E> $10^{18.6}$eV and $\theta < 56^\circ$.

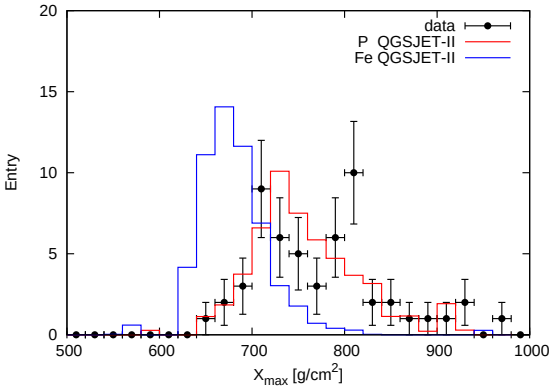

Figure 8: Distribution of X_{max} obtained from FD stereo events for E> $10^{18.6}$eV. A Preliminary Result.

A total of 54 events is selected from the data collected for November 2007 – October 2009. A set of MC events was generated using CORSIKA with an energy spectrum of $E^{-3.1}$ for the proton and iron primaries and with interaction models of QGSJET and

Sibyll. The MC events went through the same reconstruction and selection programs, and the observables were checked between the data and the MC.

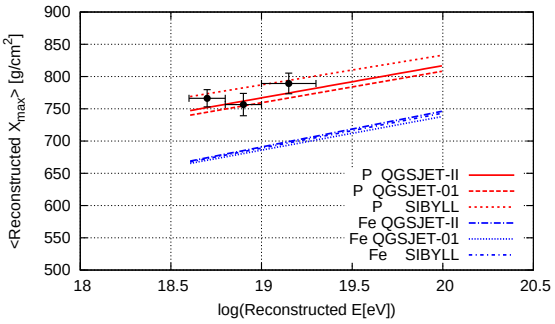

Figure 9: Energy dependence of measured X_{max}. Expectations from MCs with proton and iron primaries are given. A Preliminary Result.

The distribution of X_{max} is plotted in Fig.8 together with the expectation from the MC for proton and iron primaries. The change of average X_{max} with energy is plotted in Fig.9. Note that the value of X_{max} contains a small systematic bias originating from the event reconstruction and the selection. The comparison was made in Figs.8 and 9 with these biases kept un-removed both in the data and the MC. It can be seen from these figures that the composition of UHECR is consistent with proton and unchanged for energies higher than $10^{18.6}$eV.

Acknowledgments

The construction and operation of TA is supported by the Japanese government (MEXT) through the "Kakenhi" grant and by the U.S. funding of the National Science Foundation. The support by the Korea Research Foundation, the Korean Science and Engineering Foundation, the Russian Academy of Sciences and Belgian Science Policy are acknowledged. We thank the State of Utah School and Institutional Trust Lands Administration (SITLA), the Bureau of Land Management (BLM), and the United States Air Force. We wish to thank people and officials of Millard County, Utah, for their warm and steadfast supports of TA.

References

[1] K.Greisen, Phys. Rev. Lett. **16**, 748 (1966); T.Zatsepin and V.A.Kuzmin, JETP Lett. **4**, 78 (1966).
[2] N.Chiba *et al.*, Nucl. Instr. and Methods **A311**, 338 (1992).
[3] M.Takeda *et al.*, Phys. Rev. Lett. **81**, 1163 (1998).
[4] M.Takeda *et al.*, Astropart. Phys. **19**, 447 (2003).
[5] T.Abu-Zayyad *et al.*, Nucl. Instr. and Methods **A450**, 253 (2000).
[6] T.Abu-Zayyad *et al.*, Phys. Rev. Lett. **92**, 151101 (2004); T.Abu-Zayyad *et al.*, Astropart. Phys. **23**, 157 (2005); R.U.Abbasi *et al.*, Phys. Rev. Lett. **100**, 101101 (2008).
[7] The Telescope Array Project Design Report, July, 2000.
[8] J.Abraham *et al.*, Nucl. Instr. and Methods **A523**(2004) 50.
[9] J.Abraham *et al.*, Phys. Rev. Lett. **101**, 061101 (2008).
[10] Y.Tameda *et al.*, Nucl. Instr. and Methods **A609**, 227 (2009).
[11] H.Tokuno *et al.*, Nucl. Instr. and Methods **A601**, 364 (2009).
[12] T.Shibata *et al.*, Nucl. Instr. and Methods **A597**, 61(2008).
[13] A doctor thesis by D.Ikeda, University of Tokyo, 2010.
[14] A doctor thesis by Y.Tameda, Tokyo Institute of Technology, 2010.
[15] R.U.Abbasi *et al.*, Astropart. Phys. **29**, 77 (2007).
[16] F.Kakimoto *et al.*, Nucl. Instr. and Methods **A372**, 527 (1996).
[17] H.Sagawa *et al.*, Proceedings of the 31st International Cosmic Ray Conference, 2009, Łódź, Poland.